

Ultrasound propagation in diploe of swine skull

ブタ頭蓋骨板間層中の超音波伝搬

Itsuki Michimoto[‡], Takashi Misaki, Tsukasa Nakamura, Mami Matsukawa
(Doshisha University, Kyoto, Japan)

道本 樹[‡], 見崎 貴史, 中村 司, 松川 真美 (同志社大学)

1. Introduction

Recently, ultrasound techniques attract attention as one of the brain treatment and diagnosis methods for brain diseases such as essential tremor, neuralgia and brain tumor[1]. In these techniques, ultrasound waves are irradiated from outside of the head and enter the brain through the skull. The skull mainly consists of trilaminar, outer, diploe and inner, which are all heterogeneous and anisotropic[2]. Therefore, we should consider the complicated ultrasound propagation in the skull for more effective treatment in the brain therapy. In this study, we investigated ultrasound propagation characteristics in the thickness direction of the diploe experimentally.

2. Specimen preparation

A specimen was fabricated from a swine skull, which was similar in size to the human skull. The specimen has rectangular shape (10.0×10.0×8.0 mm³) and was obtained from the left posterior diploe (Fig. 1). The cancellous structure of the diploe was observed by an X-ray micro-computed tomography (micro-CT) system (SMX-160CTS, Shimadzu, Kyoto). We then obtained a 3D reconstructed image of the trabecular structure. Structural parameters of the specimen were estimated from the images using a software (TRI/3D-BON, RATOC, Tokyo). They were BV/TV (Bone Volume fraction: Bone Volume / Total Volume), MTA (Main Trabecular Alignment direction), MIL (Mean Intercept Length), DA (The Degree of Anisotropy) (Table 1). MIL and angles θ and φ were defined as shown in Fig. 2.

BV/TV in the swine skull was larger than those in the human and bovine femur (15-35 %) [3] as shown in Fig. 3.

For the ultrasonic measurements, the samples were degassed in water for 3 hours to remove any air bubbles inside.

3. Ultrasound measurements

Figure 3 shows the experimental ultrasonic pulse immersion system, to observe the longitudinal wave which passed through the specimen in water. A single sinusoidal wave from 0.5 MHz to 2.0 MHz with amplitude of 7 V_{p-p} was delivered from a function generator (33250A, Agilent Technologies, Colorado) and sent to the power amplifier (HAS 4101, NF, Yokohama). This signal was applied to a PVDF focused transmitter (Toray Engineering, Yokohama,

custom made: 20 mm in diameter with a focal length of 40 mm) for ultrasound radiation. The longitudinal waves which passed through the sample were received by the other PVDF flat receiver (hand-made, 3 mm in diameter) and the waveforms were observed by an oscilloscope (DPO 3054, Tektronix, Tokyo)

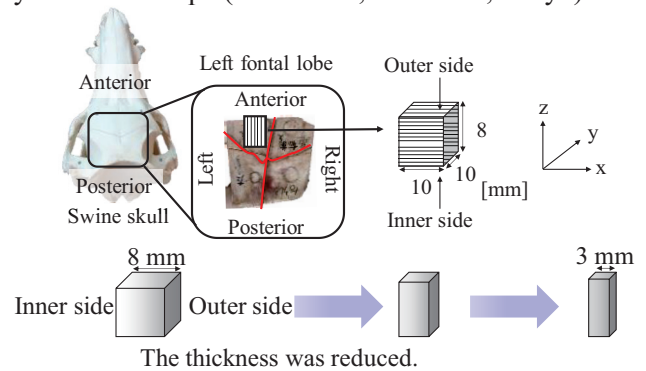


Fig. 1 Swine specimen.

Table 1 MTA and DA of the specimen.

	MIL a	MIL b	MIL c
length [mm]	0.446	0.356	0.276
θ [deg.]	86.2	175.1	93.1
φ [deg.]	-65.3	75.0	-155.4
DA	1.61		

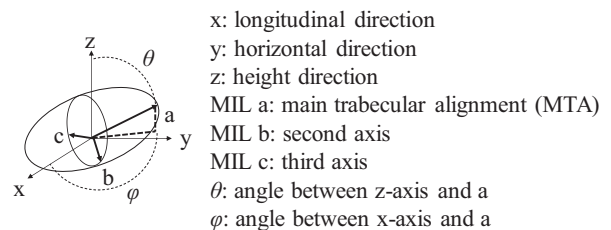


Fig. 2 MIL ellipsoid.

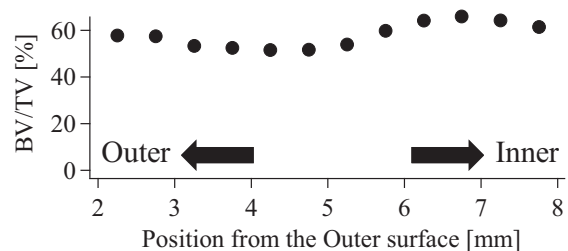


Fig. 3 The relationship between position and BV/TV of specimen.

after the amplification (BX-31A, NF, Yokohama).

The specimen was then shortened by 0.5 mm, and the measurements were repeated, from the thicknesses of 8.0 mm to 2.0 mm.

4. Result and Discussion

Figure 5 shows an observed waveform propagated in the specimen and water, and propagated in water only. In this specimen, the second axis (MIL b) almost aligned in the thickness direction.

We defined arrival time T_t from the position 10 % of the first peak amplitude at each specimen thickness.

Figure 6 shows apparent frequency f of observed waves. The apparent frequency was defined from the arrival time of first peak T_t and the time at the maximum amplitude of the first peak T_p to avoid the influences of scattering and multiple reflections.

$$f = \frac{1}{4(T_p - T_t)} \quad (1)$$

The apparent frequency was higher in thin specimens less than 4.0 mm. On the other hand, apparent frequencies were almost constant in specimens with thickness over 5.0 mm. The tendency was similar in all data of the radiated waves at different frequencies. Fujita et. al., have reported that the apparent frequency also became almost constant in equine cancellous bone [4].

Then we calculated apparent attenuation in each part of the specimen. The apparent attenuation was defined by

$$\alpha = \left\{ 20 \log_{10} \left(\frac{V_{n+1}}{V_n} \right) \right\} / \Delta d \quad (2)$$

where V_n and V_{n+1} are the amplitudes of the peaks in the received waveforms. The indices n and $n+1$ correspond to successive sample thicknesses differing by Δd (0.5 mm). Then, the obtained value shows the attenuation in the small portion of the specimens.

Figure 7 shows attenuation data. Changes of attenuation were similar to the tendency of apparent frequency and became almost constant in thick specimens. Attenuation seemed higher in the specimen thinner than 4.0 mm.

Conclusion

In this study, we investigated ultrasound propagation in the thickness direction of the swine skull diploe. As a result, we confirmed that ultrasound propagates characteristically in the thickness direction.

Reference

1. M. S. Canney, et. al., J. Acoust. Soc. Am., vol. 124, No. 4, pp.2406-2420, 2008.
2. S. A. Goss, et. al., J. Acoust. Soc. Am. Vol. 64, No. 2, pp.423-457, 1978.
3. K. Mizuno, et. al., J. Acoust. Soc. Am., Vol. 125, No. 5, p. 3464, 2009.

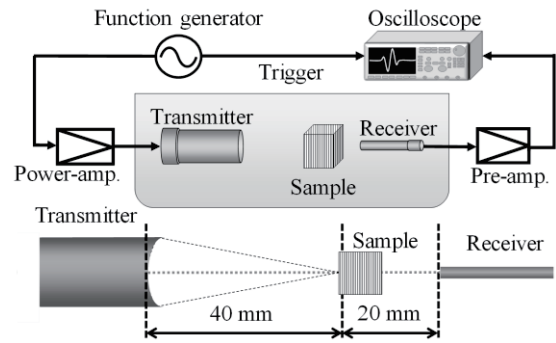


Fig. 4 Measurement system.

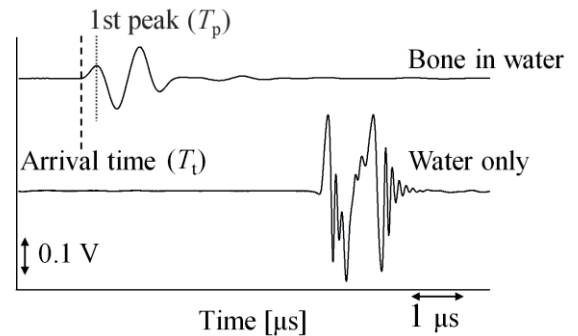


Fig. 5 Observed waveform at 1 MHz which passed through the specimen with the thickness of 2.0 mm.

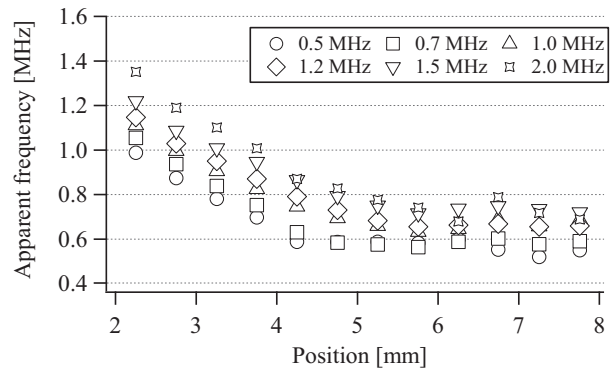


Fig. 6 The relationship between position and apparent frequency.

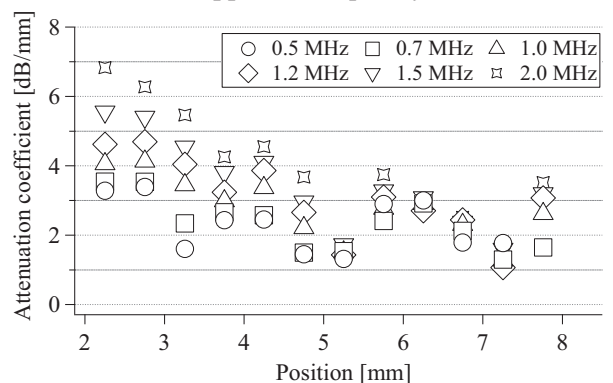


Fig. 7 The relationship between position and attenuation.

4. F. Fujita, et. al., J. Acoust. Soc. Am., Vol. 134, No. 6, p.4778, 2013.
5. Y. Nagatani, et. al., Ultrasonics, Vol. 48, pp. 607-612, 2008.